Bojana M. Radojković[1], Bore V. Jegdić[1], Biljana M. Bobić[1], Slavica Ristić[2], Suzana Polić[2]*

[1]University of Belgrade, Institute of Chemistry, Technology and Metallurgy, Belgrade, Serbia, [2]Central Institute for Conservation in Belgrade, Belgrade, Serbia

Scientific paper
ISSN 0351-9465, E-ISSN 2466-2585
UDC:628.147.22:66.088: 661.872
doi:10.5937/zasmat2001041R

Zastita Materijala 61 (1)
41 - 51 (2020)

Corrosion characteristics of laser-cleaned surfaces on iron artefact**

ABSTRACT

Nd:YAG laser was used for cleaning surfaces of cultural heritage iron artefacts covered with corrosion products. The corrosion products were removed without damaging the base material. Three different electrochemical techniques were used for the determination of the corrosion rate of mechanically prepared iron, laser-cleaned iron and laser-cleaned iron with Paraloid B44 coating. The morphology of the tested surfaces was analysed by SEM. The linear polarization resistance technique, electrochemical impedance spectroscopy and linear sweep voltammetry have shown that the corrosion rate of the laser-cleaned iron is approximately 50 % higher than the corrosion rate of the mechanically prepared iron. Electrochemical impedance spectroscopy has shown that the pore resistance of the Paraloid coating on the laser-cleaned iron sample decreases at the beginning of the test and remains approximately constant after this period. At the beginning of the test, the charge transfer resistance value is constant and then decreases rapidly i.e. the corrosion rate of the iron in the Paraloid coating pores increases with time. During the linear sweep voltammetry test of the iron sample with Paraloid coating, it was noticed that the anodic polarisation curve shows an unusual shape at the potentials more positive than - 0.5 V.

Keywords: *Iron artefacts, laser-cleaning, corrosion, electrochemical techniques, corrosion rate.*

1. INTRODUCTION

Iron and steel corrode uniformly in neutral and slightly acidic environments, usually present in the depots with cultural heritage artefacts. The quantitative indicator of general uniform corrosion is the corrosion rate. Different factors can affect corrosion of iron artefacts. Surface treatments and protective coatings can significantly influence the corrosion process rate [1-4].

In recent years, lasers have been increasingly used in the processing of metals. Lasers can be used for cutting, drilling, marking, engraving, cleaning, welding and other operations [5-9]. The advantages of laser application in metal processing are significant: the process is contactless, precise and fast, and does not cause deformation in the material [10].

One of the major advantages of laser as a tool for material processing is a possibility to precisely control the quantity of energy deposited on the determined place on the material surface. This control is realised through a proper selection of laser processing parameters, which leads to desired material modifications, laser surface cleaning and laser coating removal [10,11].

Besides the fact that lasers have been widely used in metal surface processing, the changes that occur on laser treated metal surfaces have not been sufficiently investigated yet. Changes in the structural, chemical and mechanical properties, changes in the rate of corrosion, corrosion resistance and others similar characteristics have not been studied in detail. Therefore, it is of interest to study these properties of laser treated material surfaces and to choose the laser beam parameters that will result in the desired changes.

Nowadays, lasers are widely used in different tests, analyses, monitoring, and conservation of industrial and cultural heritage objects. Over the past 50 years, cultural heritage conservation has been developed into a professional skill using the latest scientific methods. Lasers are used in removal of corrosion products on corroded metal artefacts [12-17].

*Corresponding author: Bojana Radojkovic
E-mail: bojana.radojkovic@ihtm.bg.ac.rs

Paper received: 10. 11. 2019.
Paper accepted: 04. 12. 2019.
Paper is available on the website: www.idk.org.rs/journal
**The Manuscript is presented at 21st YuCORR conference on Tara Mountain, 17-20 September 2019.

Corrosion is a problem for all metallic heritage artefacts. The conventional techniques of metal surface cleaning are based on mechanical or chemical methods which can lead to the substrate being damaged or polluted. Laser cleaning is of interest due to its great potential for removing contamination or films from different substrates. The cleaning of oxidized iron specimens at different laser spot sizes was performed using different pulse numbers at λ=1064 nm and λ=532 nm [10,18].

In the protection of metal surfaces, especially in the conservation of cultural heritage objects, Paraloid B44 acrylic coating is very often used. Incralac, a commercial coating for metals, contains Paraloid B44 as an important component. It is colourless thermoplastic acrylic resin, which has been used for protection both organic and inorganic materials. Paraloid B44 can be applied to archaeological objects as well as on clean metal surfaces [19].

Laser application in metal cleaning includes the laser–metal interaction and it is specific for every type of metal. The material surface reflects the part of light that strikes it due to the difference in the real refraction index. The rest of light energy is transmitted into the material the surface roughness of which can cause multiple reflections involving multiple absorption events. This can result in very high local absorbance levels. The electromagnetic energy of the absorbed laser light has to be transformed into thermal energy inside the metal. The amount of the transformed energy depends on the light absorption mechanisms in the metal. The reflectivity of metals in the near UV and visible spectral range is typically between 0.4 and 0.95, while for the IR spectra, it is between 0.9 and 0.99 [5]. A part of incidence laser energy enters the material; absorption causes the light intensity to decrease with depth at a rate determined by the material's absorption coefficient.

The surfaces of cultural heritage artefacts and conventional metals kept in air are most often covered with oxide layers that sometimes show a multilayer structure. Oxide layers can cause an increase in sample absorptivity. The variation of absorptivity with temperature is of great practical importance in laser surface cleaning.

The laser beam can interact with the sample metal surface and the impurities on it, producing various effects such as ablation of corrosion products. The exact nature of material ablation by laser irradiation depends on the used material and the laser processing parameters. Surface cleaning, based on laser ablation, is an irreversible process, followed by many potential complications. It is very important to choose the most suitable laser cleaning methodology and laser parameters depending on the material properties. As a result of the cleaning effect, modifications of the surface properties (hardness, corrosion or wear resistance, adhesion, etc.) may be expected.

The aim of this paper was to examine the corrosion resistance of the laser treated surface of iron artefacts with and without Paraloid B44 protective conservation coating. The changes in the corrosion resistance of the iron plate after laser cleaning by Nd:YAG laser (λ ≈ 1064 nm) were studied. The results of the corrosion resistance testing of the mechanically prepared iron surface are presented as well as the results obtained from the laser-cleaned iron with and without Paraloid B44 conservation coating. The corrosion tests were performed using various electrochemical techniques: linear polarization resistance (LPR), electrochemical impedance spectroscopy (EIS) and linear sweep voltammetry (LSV). As a result of the electrochemical measurements, the charge transfer resistance and the corrosion current density were obtained, which can be expressed as the corrosion rate. The corrosion rate was determined in a solution containing chlorides and sulphates, i.e. in a moderately acidic solution. This solution simulates more severe conditions of exploitations than those in museums or their depots. The used electrochemical methods have provided very useful information about corrosion behaviour of iron artefacts after laser cleaning process and conservation with protective Paraloid B44 coating.

2. EXPERIMENTAL PART

Nd:YAG laser, Thunder Art Laser, produced by Quanta System (with wavelengths λ = 1064 or λ = 532 nm, optical pulse duration < 8 ns, and output pulse energy up to 1000 mJ) was used in the presented experiments. The repetition rate is up to 20 Hz, with a beam diameter of 10 mm and 70 % fit to Gaussian energy distribution. All experiments were performed on a 3 mm thick iron plate. The iron sample, used in this test, was covered with corrosion products.

The laser parameters used for two cleaning zones were: λ = 1064 nm, the energy E = 750 mJ (fluence 3.8 J/cm^2), the number of pulses n = 500, and the laser spot diameter d=5mm. The specimen was placed in front of the laser head so that the laser beam was directed perpendicularly to the specimen. A dry cleaning method was used. The experiment was performed in atmospheric conditions.

One of the treated zones was coated with clear (transparent) Paraloid B44 protective coating (25 %

in acetone) in a relatively uniform layer using a fine brush.

A scanning electron microscope (SEM) JEOL JSM-6610LV, which operates at 20 kV, equipped for energy dispersive spectroscopy (EDS) measurements, was used to analyse the morphology of the laser treated steel surface with and without Paraloid B44 protective coating. The same SEM/EDS device was used for the analysis of the chemical composition of the iron surfaces.

The chemical composition of the tested iron sample (base metal) is given in Table 1.

Table 1. Chemical composition of the tested iron (base metal)

Tabela 1. Hemijski sastav ispitivanog gvožđa (osnovni metal)

Element	C	Mn	Si	Fe
Mass. %	2.74	0.34	0.18	rest

The corrosion resistance of the mechanically prepared iron sample as well as that of the laser cleaned samples (with and without Paraloid B44 protective coating) were studied applying three electrochemical techniques.

2.1 Electrochemical techniques

The following electrochemical techniques were applied: linear polarization resistance (LPR), electrochemical impedance spectroscopy (EIS), and linear sweep voltammetry (LSV).

2.1.1 Linear polarization resistance technique

This technique was used to determine the polarization resistance (or the charge-transfer resistance R_{ct}) of the tested iron sample in the corrosion environment (test solution). The value of R_{ct} is inversely proportional to the corrosion current density j_{corr} and to the corrosion rate v_{corr} [20,21]. The iron sample was polarized in a narrow potential range (E = ± 10 mV) with respect to the corrosion potential E_{corr}, starting from the cathodic region to the anodic one, and then the corresponding current j was recorded. The potential sweep rate was 0.166 mVs^{-1}. The value of R_{ct} was determined as the slope of the experimental E - j curve at the corrosion potential E_{corr}. The corrosion current density j_{corr} was calculated using the experimentally determined value of R_{ct}.

2.1.2 Electrochemical impedance spectroscopy

The value of R_{ct} was also determined using the EIS technique [22]. Alternating potential of a small amplitude (± 10 mV) was imposed on the working electrode (the tested iron sample) in the test solution. The applied frequencies f were from 100 000 Hz to 0.01 Hz. The value of R_{ct} was determined on the basis of the electrochemical impedance values at very high and very low frequencies. The corrosion current density and the corrosion rate were then calculated using the experimental value of R_{ct}. The corrosion current density j_{corr} was calculated using the Stern-Geary equation:

$$j_{corr} = B/R_{ct} \quad (1)$$

where B is a constant that depends on the values of theTafel slopes (b_a and b_c):

$$B = b_a \cdot b_c / 2.303 \cdot (b_a + b_c) \quad (2)$$

The value of the constant B for the tested iron sample in NaCl + Na_2SO_4 (pH3) solution is ~ 17 mV [23]. According to equation (1), the corrosion current density j_{corr} is:

$$j_{corr} = 17\ mV / R_{ct} \quad (3)$$

The corrosion rate v_{corr} can be calculated using the Faraday law, based on the corrosion current density j_{corr}, in accordance with ASTM G102 [24].

2.1.3 Linear sweep voltammetry

This technique was used to obtain the Tafel polarisation diagrams [25]. The iron sample was polarized in the potential range E = ± 0.200 V relative to E_{corr} and the corresponding current density j was recorded. The applied potential sweep rate was 1 mVs^{-1}. The corrosion current density j_{corr} was directly determined from the obtained Tafel diagrams by extrapolating the linear parts of the anodic and cathodic polarization curves to the corrosion potential E_{corr}.

The electrochemical tests were carried out using a potentiostat/galvanostat Biologic SP-200, in a solution containing sulphates and chlorides (0.3 mol dm^{-3} NaCl + 0.1 mol dm^{-3} Na_2SO_4). H_2SO_4 was added to the test solution to achieve the desired pH value (pH3). The tests were performed at room temperature, in the presence of atmospheric oxygen.

The tests were carried out in an electrochemical cell with a saturated calomel electrode (SCE) as a reference electrode and a Pt mesh as an auxiliary electrode. The working electrode was the mechanically prepared iron sample and laser-cleaned iron sample, with and without Paraloid B44 conservation coating. Before the beginning of the polarization measurements, the sample was kept for a certain time period at open circuit potential, to establish a stable corrosion potential E_{corr}.

3. RESULTS AND DISCUSSION

3.1. Laser cleaning results

The corrosion layer cleaning from a metal sample by laser irradiation is a complex phenomenon. As mentioned before, it is based on several processes: absorption of laser energy within several nano seconds, melting of the material in the heated layer depending on the applied energy, and material ablation or evaporation. Depending on the fluence and the quantity of the absorbed energy, mechanical expansion waves consisting of evaporated material and ambient gas can be formed in the vicinity of the sample surface; they also remove parts of the surface layers and discard them from the irradiated zone. The laser beam can induce chemical, structural and morphological modifications, leading to a change in the surface characteristics.

High resolution images of the treated and untreated zones on the sample surface were obtained by scanning electron microscopy (SEM). The laser irradiation results were observed and analysed.

Figures 1a present the SEM images of the laser-untreated iron surface at different magnify-cations. It can be seen that the sample is covered with a layer of corrosion products. The corrosion products cover the entire sample surface and have a grain-like shape. The dimensions of the grains are approximately 2 - 5 μm.

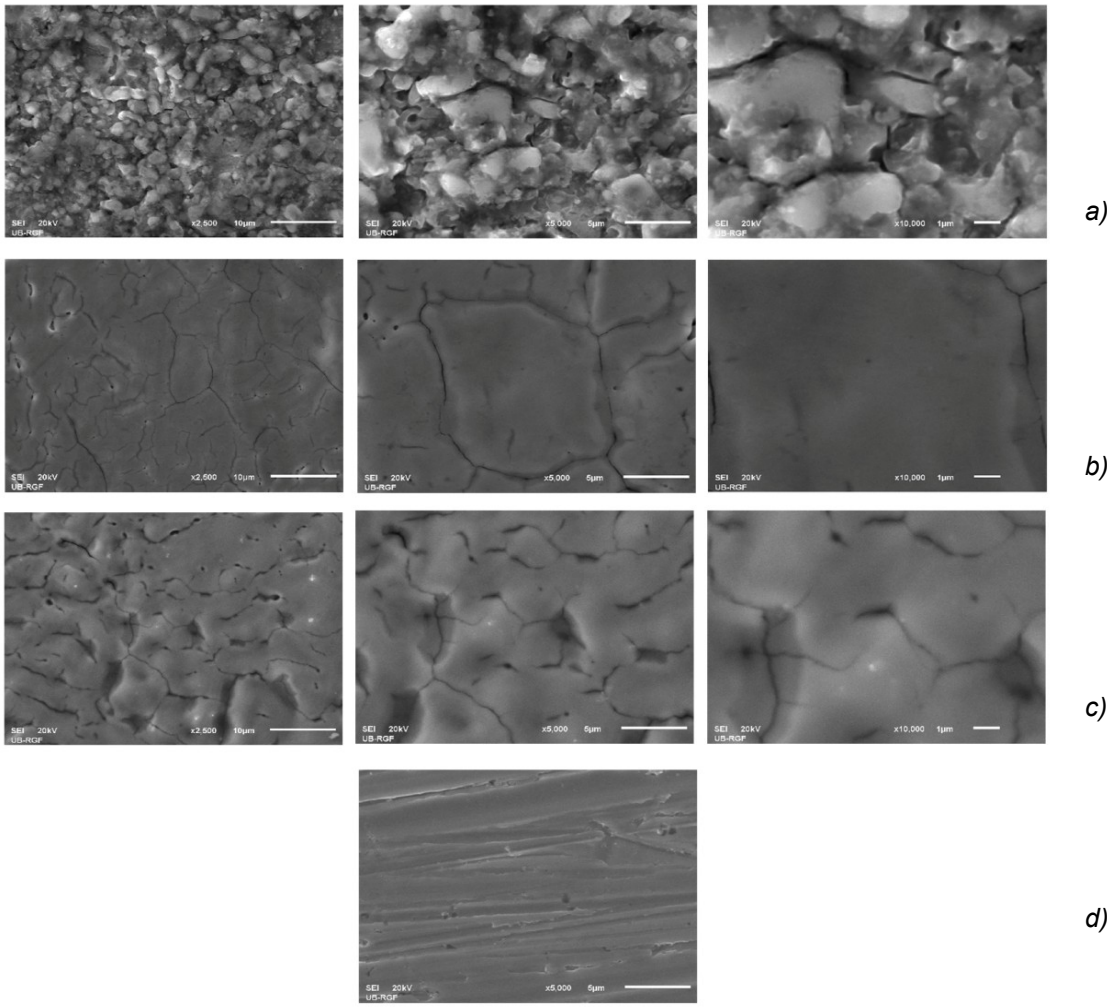

Figure 1. SEM micrographs of the a) laser-untreated iron sample, covered with corrosion products, b) laser-cleaned zone of the iron sample, c) laser-cleaned zone of the iron sample with Paraloid B44 coating and d) mechanically prepared iron surface

Slika 1. SEM mikrofotografije a) uzorak gvožđa prekriven korozionim produktima, b) laserski očišćena površina na uzorku od gvožđa, c) laserski očišćena površina na uzorku od gvožđa sa prevlakom Paraloid B44 i d) mehanički pripremljena površina gvožđa

Figure 1b illustrates the topography of the zone on the iron sample surface after laser irradiation. It can be seen that all corrosion products have been removed in the central part of the laser-cleaned zone.

The macroscopic analysis of the tested sample (Figure 1b) shows that the applied laser fluence caused visible changes. The chosen parameters of corrosion products cleaning are below the damage threshold of iron. The laser beam caused the removal of corrosion products without damaging the base material.

When using Nd:YAG lasers for corrosion cleaning, correct operating parameters have to be chosen. The corroded surface may become darker at high-energy densities and/or after several pulses. The use of pulsed near-infrared Nd:YAG lasers for cleaning corroded metals may be limited by the risk of surface melting and blackening due to thermal and photo-chemical changes [12].

The SEM images of the laser-cleaned zone with Paraloid B44 coating are presented in Figure 1c. The coating was applied in a thin layer on the laser-cleaned iron surface. The coating follows the surface topology.

Electrochemical corrosion testing was also performed on the mechanically prepared iron surface with the aim of comparing its corrosion resistance with the corrosion resistance of the laser-cleaned iron zone. Figure 1d shows the iron surface after mechanical cleaning and degreasing. The traces of the previous mechanical grinding can be seen.

3.2. Results of electrochemical tests

3.2.1. Mechanically prepared iron sample and laser-cleaned iron sample

Corrosion on iron artefacts in moderately acidic solutions in the presence of chlorides and sulphates is a complex electrochemical process that consists of several anodic and cathodic reactions.

In moderately acidic solutions, the main anodic reaction is oxidation of iron to the bivalent state (Fe^{2+}) with the release of electrons:

$$Fe = Fe^{2+} + 2e^{-} \quad (4)$$

The main cathodic reaction is hydrogen evoluation:

$$2H^{+} + 2e^{-} = H_2 \quad (5)$$

Due to the presence of atmospheric oxygen, cathodic oxygen reduction also takes place:

$$O_2 + 4H^{+} + 4e^{-} \rightarrow 2H_2O \quad (6)$$

The cathodic reaction of water reduction, although thermodynamically possible, occurs at a very low rate and can practically be neglected.

Figure 2 shows the results obtained using the linear polarization resistance method on the mechanically prepared iron sample (Figure 2a) and on the laser-cleaned iron sample (Figure 2b).

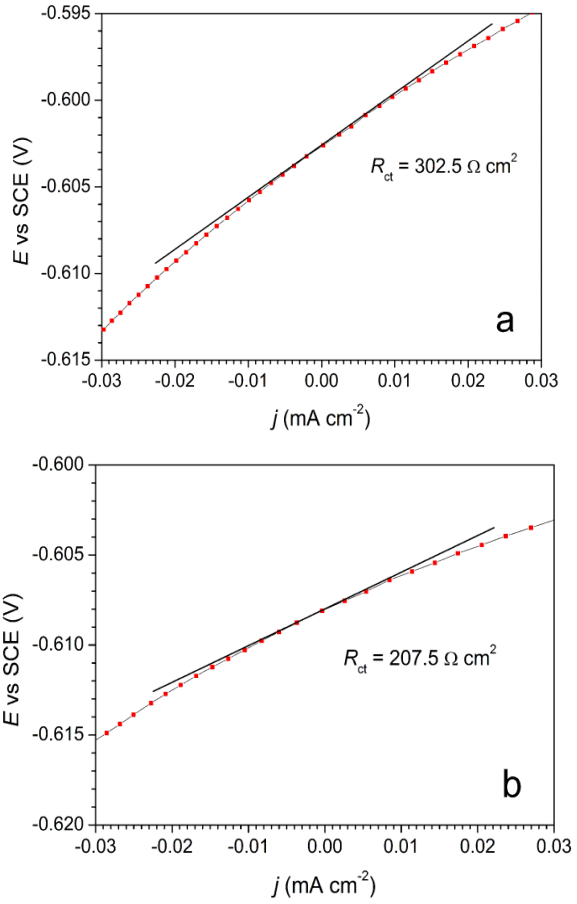

Figure 2. Results of the LPR tests: a) mechanically prepared iron and b) laser-cleaned iron

Slika 2. Rezultati ispitivanja LPR metodom: a) mehanički pripremljena površina gvožđa i b) laserski očišćena površina gvožđa

The slope of the experimental potential-current density E - j curve on the corrosion potential E_{corr} represents the value of the charge transfer resistance R_{ct}. The R_{ct} value for the mechanically prepared iron sample is 302.5 Ω cm^2, which is approximately 46 % higher than the R_{ct} value for the laser-cleaned iron sample (R_{ct} = 207.5 Ω cm^2). Based on the R_{ct} values, the corrosion current density j_{corr} (Equation 3) and the corrosion rate v_{corr} of the iron samples were calculated using ASTM G102 standard [24]. The corrosion rate v_{corr} of the laser-cleaned iron sample is also approximately 46 % higher than the corrosion rate v_{corr} of the mechanically treated iron sample.

Figures 3 and 4 show the results obtained by the method of electrochemical impedance spectroscopy on the mechanically prepared iron sample and the laser-cleaned iron sample.

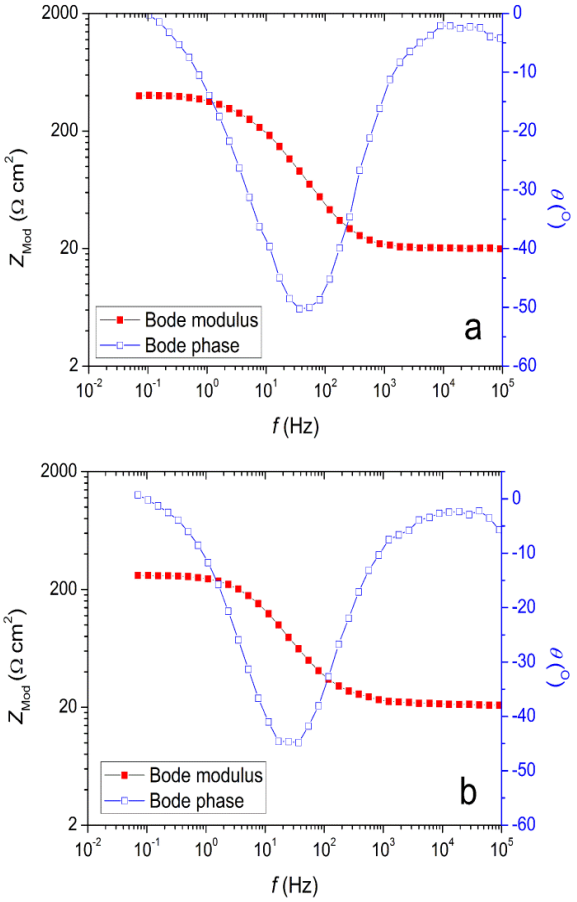

Figure 3. Results of the EIS tests (the Bode modulus and the Bode phase diagrams): a) mechanically prepared iron and b) laser-cleaned iron

Slika 3. Rezultati ispitivanja EIS metodom (Bode moduo i Bode fazni dijagrami): a) mehanički pripremljena površina gvožđa i b) laserski očišćena površina gvožđa

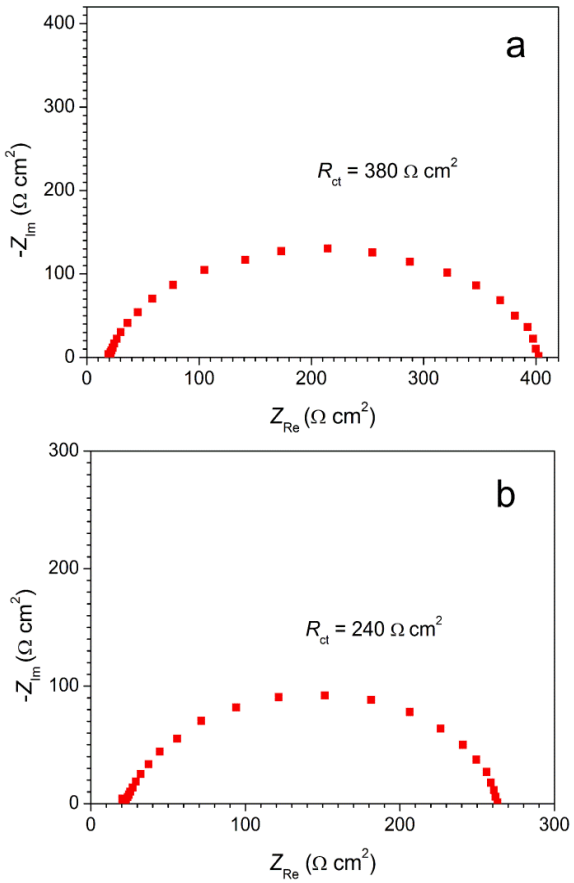

Figure 4. Results of the EIS tests (the Nyqist plots): a) mechanically prepared iron and b) laser-cleaned iron

Slika 4. Rezultati ispitivanja EIS metodom (Nyquist-ovi dijagrami): a) mehanički pripremljena površina gvožđa i b) laserski očišćena površina gvožđa

Figure 3 shows the obtained Bode plots (the Bode modulus and the Bode phase diagram), while Figure 4 shows the Nyquist plots. The charge transfer resistance R_{ct} value is obtained as the difference of impedance values at low and high frequencies. The R_{ct} value for the laser-cleaned iron sample is 240 Ω cm^2, while the R_{ct} value for the mechanically prepared iron sample is 380 Ω cm^2. The results of the EIS measurements show that the value of the charge transfer resistance R_{ct} for the laser-cleaned sample is about 58 % higher than the value of R_{ct} for the mechanically prepared iron sample. The values of the corrosion current density j_{corr} and the corrosion rate v_{corr} were calculated using the obtained R_{ct} values.

Figure 5 shows the results obtained using the linear sweep voltammetry method (the Tafel diagrams). The results for the mechanically prepared iron sample and the laser-cleaned iron sample are shown in this figure. The value of the corrosion current density j_{corr} is determined by the extrapolation of the linear parts of the anodic and cathodic polarisation curves to the corrosion potential E_{corr}. The value of the corrosion current density j_{corr} is about 30 % higher for the mechanically prepared iron sample than for the laser-cleaned iron sample. The value of the corrosion rate v_{corr} is directly proportional to the value of the corrosion current density j_{corr} [24].

The results presented show that all three electrochemical methods give the same results (Figures 2-5). The corrosion rate of the laser-cleaned iron sample is about 50 % higher than the corrosion rate of the mechanically prepared iron sample

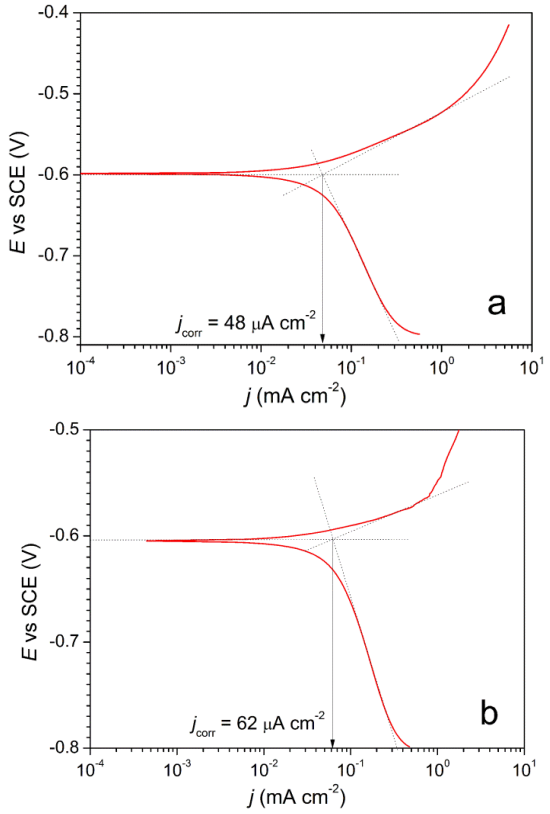

Figure 5. Results of the LSV tests (the Tafel plots): a) mechanically prepared iron and b) laser-cleaned iron

Slika 5. Rezultati ispitivanja LSV metodom (Tafel-ovi dijagrami): a) mehanički pripremljena površina gvožđa i b) laserski očišćena površina gvožđa

This unusual behaviour of iron can be explained as follows: laser treatment (cleaning) causes the local surface heating of a thin metal layer, which leads to the melting and decomposition of the previous iron matrix structure. Rapid cooling leads to various structural transformations. The formation of a fine perlite, beinite or martensite structure can occur in the surface iron layer. It is known that the presence of a fine perlite, beinite and martensite structure results in higher strength and hardening of the iron matrix. On the other hand, the rate of corrosion reactions (the rate of the cathodic reaction in particular) can be increased due to the formation of a fine perlite, beinite or martensite structure. This phenomenon, that laser-cleaned iron has a higher corrosion rate, has been previously observed and considered by other authors [26]. The morphological changes of a steel surface layer after laser treatment were analyzed in [27,28].

3.2.2. Laser-cleaned iron sample with Paraloid B44 coating

Electrochemical impedance spectroscopy has been widely used for testing corrosion resistance of iron and for testing corrosion stability of coatings on iron. In this work EIS technique is applied to study the corrosion behaviour of laser-cleaned iron surface with Paraloid B44 coating. This technique provides information about the coating itself, such as its adhesion, barrier properties, defects, as well as an insight into the destruction of the protective metal/coating system, even before coating degradation can be observed visually [29,30].

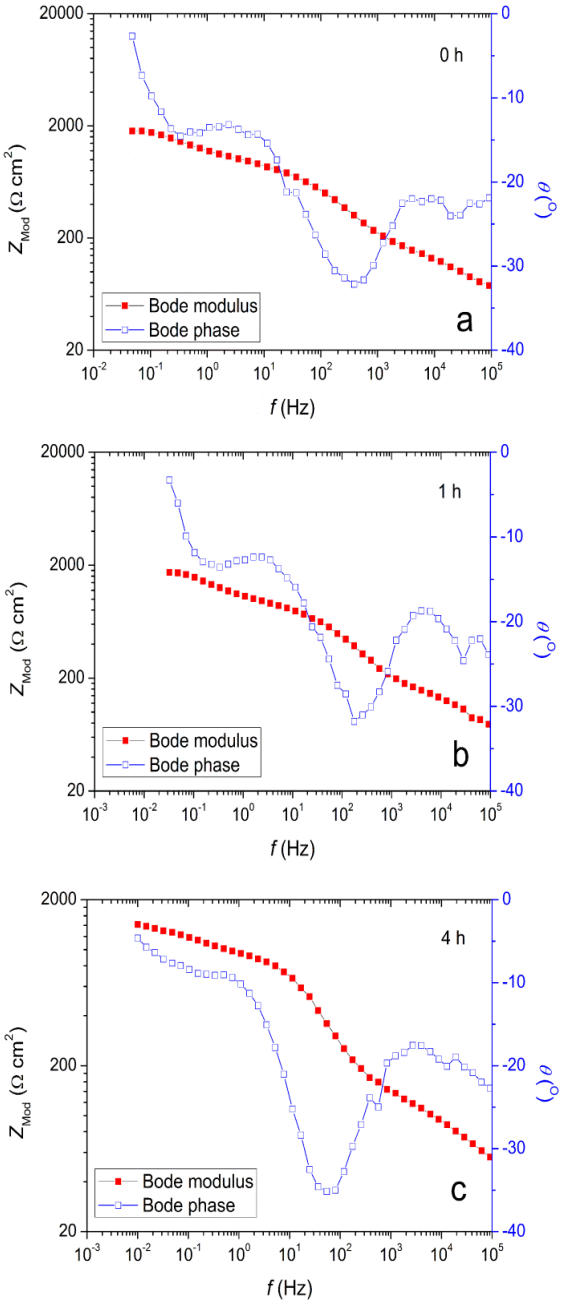

Figure 6. Results of the EIS tests (the Bode plots) for the laser-cleaned iron sample protected with Paraloid B44 coating after: a) 0 h, b) 1 h and c) 4 h

Slika 6. Rezultati ispitivanja EIS metodom (Bode-ovi dijagrami) za laserski očišćenu površinu gvožđa zaštićenu prevlakom Paraloid B44, posle: a) 0 h, b) 1 h i c) 4 h

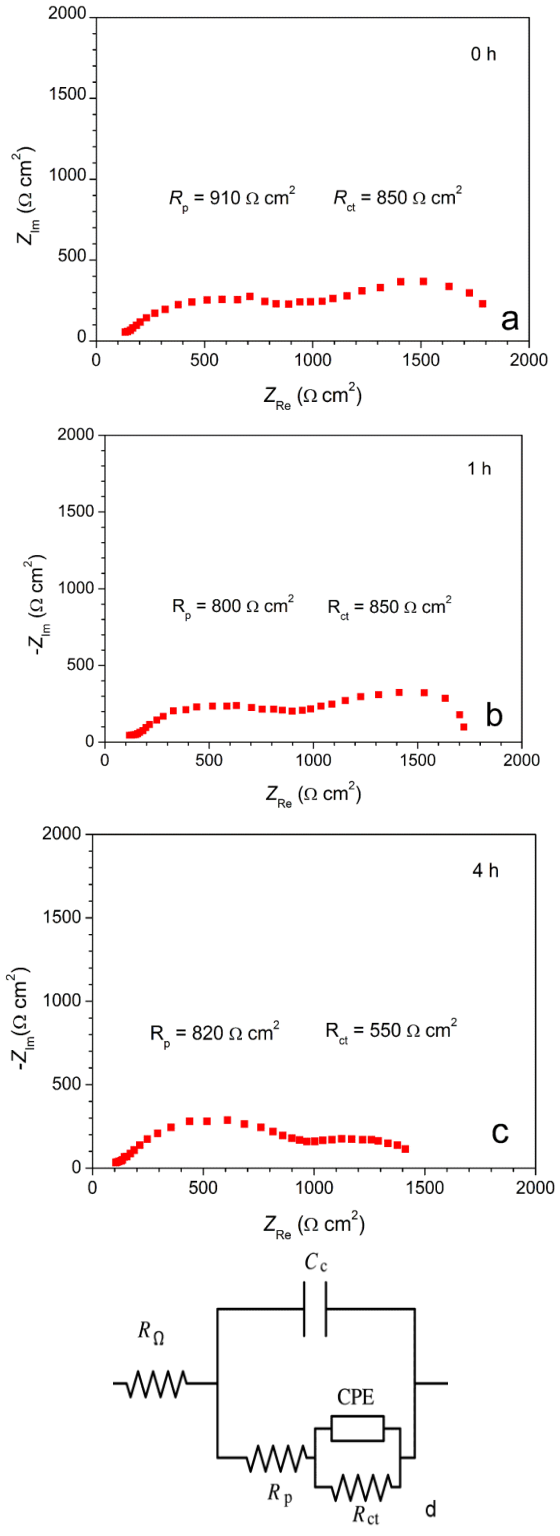

Figure 7. Results of the EIS tests (the Nyqist plots) for the laser-cleaned iron sample protected with Paraloid B44 coating after: a) 0 h, b) 1 h and c) 4 h; d) equivalent electrical circuit

Slika 7. Rezultati ispitivanja EIS metodom (Nyquist-ovi dijagrami) za laserski očišćenu površinu gvožđa zaštićenu prevlakom Paraloid B44, posle: a) 0 h, b) 1 h i c) 4 h

Figures 6 and 7 show the results of the EIS test of Paraloid B44 coating applied on the laser-cleaned iron surface.

Figure 6 shows the Bode diagrams (modulus and phase diagrams), and Figure 7 shows the Nyquist diagrams. The Bode phase diagrams show the dependence of the impedance phase angle (θ) on the logarithm of frequency (f). These diagrams are used to determine the frequency range where corrosion reactions occur, as well as for a deeper insight into the corrosion processes on protected metal.

The equivalent electrical circuit for the tested iron/Paraloid B44 coating system in the test solution is presented in Figure 7d [31]. The equivalent electrical circuit consists of the electrolyte resistance R_Ω, the coating pore resistance R_p, the coating capacitance C_c, the charge-transfer resistance R_{ct}, and a constant phase element CPE. The constant phase element CPE represents all the frequency dependent electrochemical phenomena, i.e. the double-layer capacitance C_{dl}, and diffusion processes.

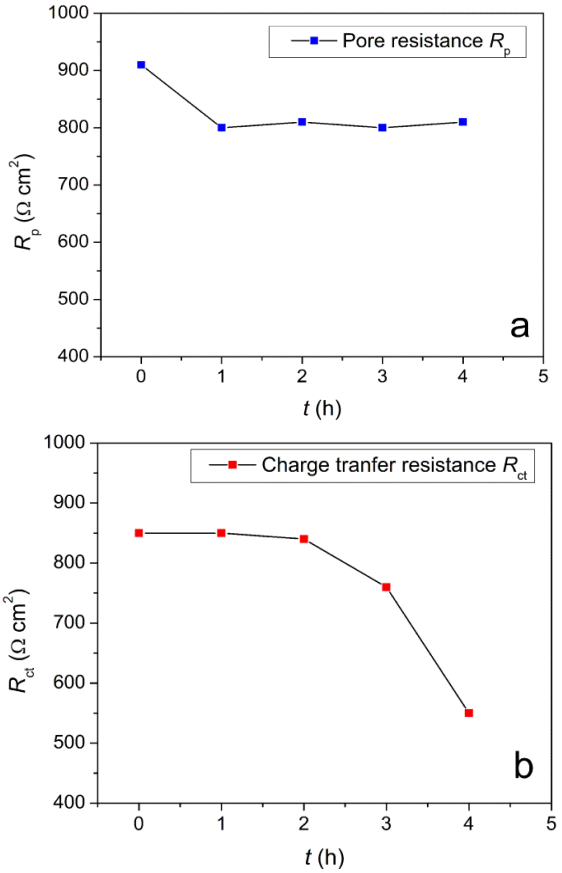

Figure 8. Time dependence: a) pore resistance Rp and b) charge transfer resistance Rct

Slika 8. Vremenska zavisnost: a) otpor elektrolita u porama prevlake Rp i b) otpor razmene naelektrisanja Rct

The pore resistance R_p decreases during the first time period (< 60 min) of the test sample exposure to the test solution (NaCl + Na_2SO_4), as a consequence of the water uptake into the Paraloid coating (Figure 8a). As the test solution keeps penetrating, at one moment it reaches the iron surface and once the electrolyte is in contact with the iron surface, the corrosion processes start. The pore resistance value R_p remains practically constant throughout the entire testing period (Figure 8a). The corrosion reactions (processes) under the Paraloid coating lead to the loss of adhesion and to partial delamination of the coating (Figure 8b) [31-33].

Two time constants appear in the EIS diagrams (Figures 6 and 7) and this electrochemical behaviour is related to the equivalent circuit shown in Figure 7d. Figures 7a-c and 8b show that the rate of the electrochemical (corrosion) reaction increases with time. The second semi-circle (Figures 7a-c) appears at different frequencies, as it can be seen on the Bode phase diagrams (Figures 6a-c).

Figure 7 shows the Nyquist plots for the Paraloid B44 coating on the laser-treated iron surface during exposure to the test solution (NaCl + Na_2SO_4). The first circle presents the pore resistance R_p, while the second circle in these figures indicates the corrosion of the iron substrate under the Paraloid coating (charge transfer resistance R_{ct}).

In the pores of the Paraloid coating (on the iron surface), several reactions take place. The electrochemical corrosion of iron, i.e. the anodic reaction of iron dissolution (Equation 4), and the cathodic reaction (Equations 5 and 6) occur. In addition, in the pores of the Paraloid coating, the pH value of the test solution decreases, due to the hydrolysis of the formed Fe^{2+} ions. The decrease in the test solution pH value increases the iron corrosion rate additionally.

It can be clearly seen that the second semi-circle in Figure 7 becomes smaller during prolonged exposure time (1 h, 2 h and 4 h), while the first semi-circle remains almost constant. As mentioned earlier, the first semi-circle (first time constant) presents the coating pore resistance (R_p) while the second semi-circle (second time constant) is related to the progress of the corrosion processes on the iron under the Paraloid coating (R_{ct}).

Figure 9 shows the Tafel plot recorded after the completion of the electrochemical impedance measurements (4 h).

The electrochemical corrosion reactions take place in the Paraloid coating pores, reaching the iron surface. The value of the corrosion current density j_{corr} is determined from the recorded Tafel plot by the extrapolation of the linear parts of the chatodic and anodic polarisation curves to the corrosion potential E_{corr}. The value of the corrosion current density j_{corr} is in accordance with the charge-transfer resistance R_{ct} value at the end of the EIS measurements (4 h). The area of the pores reaching the iron surface is considerably smaller than the surface of the test sample with the Paraloid coating (geometrical surface). Due to this, the corrosion current density in the Paraloid coating pores (j_{corr} = 18 μA cm^{-2}) is significantly lower than the corrosion current density obtained for the iron sample without Paraloid coating (j_{corr} = 62 μA cm^{-2}). In addition, the hydrolysis of metal ions (Fe^{2+}) takes place on the iron surface inside the Paraloid coating pores. This leads to a decrease in the pH value of the solution in the coating pores and to an additional increase in the iron sample corrosion rate.

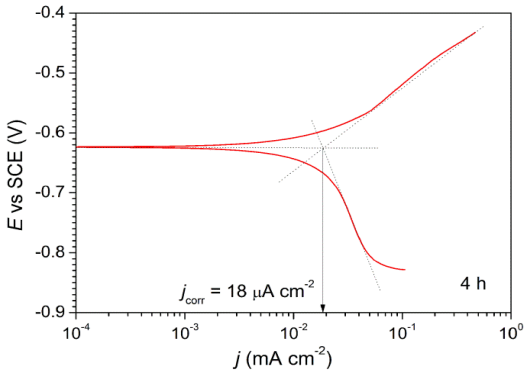

Figure 9. Tafel plot for the laser-cleaned iron sample protected with Paraloid B44 coating after 4 h

Slika 9. Tafelov dijagram za laserski očišćenu površinu gvožđa zaštićenu prevlakom Paraloid B44, posle 4h

The unusual shape of the anodic polarization curve in Figure 9, at the potentials more positive than -0.5 V, is a consequence of the corrosion processes on the iron surface below the Paraloid coating. At the potentials more positive than -0.5 V, there is significant anodic dissolution of iron under the coating, which probably leads to an additional coating delamination. The coating delamination reveals a larger iron surface that anodicaly disolves. This results in an increase of the anodic current at the potentials more positive than -0.5 V, i.e. in the unusual shape of the anodic polarisation curve (Figure 9).

4. CONCLUSION

Nd:YAG laser was used for cleaning the surface of the iron artefacts covered with corrosion products. The laser beam caused the removal of corrosion products without damaging the base material. Protective Paraloid B44 coating was applied in a thin layer on the laser-cleaned iron surface as well. The coating follows the surface topology.

The corrosion resistance of mechanically prepared iron, laser-cleaned iron, and laser-cleaned iron with Paraloid B44 coating was tested. The test was performed using three different electrochemical techniques (linear polarization resistance, electrochemical impedance spectroscopy and linear sweep voltammetry), in a solution containing chlorides and sulphates.

The obtained results have shown that the corrosion rate of the laser-cleaned iron sample is approximately 50 % higher than the corrosion rate of the mechanically prepared iron sample. This is probably caused by the structural transformation of the laser-cleaned iron sample, which led to the formation of a fine perlite, beinite or martensite structure. The corrosion rate is expected to be higher in the presence of this fine structure.

The results of electrochemical impedance spectroscopy have shown that the pore resistance R_p of the Paraloid B44 coating on the laser-cleaned iron sample decreases at the beginning of the test and remains approximately constant throughout the entire test period. On the other hand, the value of the charge transfer resistance R_{ct} is constant at the beginning of the test and then decreases rapidly. This means that the corrosion rate of the iron in the coating pores increases over time.

The value of the corrosion current density j_{corr} determined by Tafel extrapolation after the completion of the EIS test is in accordance with the value of the charge-transfer resistance R_{ct}, determined by the EIS technique.

The Paraloid B44 coating delamination at high anodic potentials during the LSV test led to the additional increase in the anodic current density, which resulted in the appearance of the unusual shape of the anodic polarisation curve at potentials more positive than - 0.5 V.

The results of this study show that it is necessary to examine all the changes occurring in the laser treated surfaces in order to ensure successful application of lasers in corrosion cleaning.

Acknowledgement

The work was financially supported by the Ministry of Education, Science and Technological Development of the Republic of Serbia, through TR 34028 and TR 35021 projects.

5. REFERENCES

[1] R.B.Griffin (2006) Corrosion in Marine Atmospheres, in: S.D. Cramer, B.S. Covino (Eds.), ASM Handbook Volume 13C, Corrosion: Environments and industries, ASM International, Ohio, p. 42-60.

[2] Z.Karastojković, S.Polić, M.Srećković, N.Ilić, Z.V. Janjušević (2017) X-Ray transparent testing of leaves from an artistic desk lamp, Zaštita materijala, 58(2), 158-162.

[3] P.R.Roberge (2008) Corrosion engineering principles and practice, McGraw-Hill, New York.

[4] Z.M.Karastojković, S.R.Polić, S.B.Čubrilović, D.N.Jovanović, Z.V.Janušević, A.S.Patarić (2018) Corrodive cracks from flux residuals after brazing of thin leaves at an artistic desk lamp, Zaštita materijala, 58(3), 454-458.

[5] H.W.Bergmann, K.Schutte, E.Schubert, A.Emmel (1995) Laser-surface processing of metals and ceramics for industrial applications, Appl. Surf. Sci., 86, 259-265.

[6] S.Ristić, S.Polić, B.Radaković, S.Linić, V.Bikić, B.Jegdić, M.Pavlović (2018) Istraživanje mogućnosti primene lasera u čišćenju arheoloških metalnih predmeta, Zaštita materijala, 58(3), 410-422.

[7] C.T.Kwok, H.C.Manc, F.T.Chengc, K.H.Lo (2016) Developments in laser-based surface engineering processes: with particular reference to protection against cavitation erosion, Surf. Coat. Tech., 291, 189–204.

[8] M.S.Brown, C.B.Arnold (2010) Fundamentals of laser-material interaction and application to multiscale surface modification, in: K.Sugioka, M.Meunier, A.Pique (Eds.), Springer Series in Materials Science 135 Laser Precision Microfabrication, Springer-Verlag Berlin Heidelberg, Berlin, p. 91-120.

[9] H.Hügel, F.Dausinger (2004) Fundamentals of laser-induced processes, in: R.Poprawe, H.Weber, G.Herziger (Eds.), Laser Physics and Applications: Laser Applications, Springer-Verlag Berlin Heidelberg, p. 3-25.

[10] P.Meja, M.Autric, P.Alloncle, P.Pasquet, R.Oltra, J.P.Boquillon (1999) Laser cleaning of oxidized iron samples: The influence of wavelength and environment, Appl. Phys. A-Mater., 69,S687–S690.

[11] J.D.Majumdar, I.Manna (2003) Laser processing of materials, Sadhana-Acad. P. Eng. S., 28, 495–562.

[12] Y.Koh, I.Sárady (2003) Cleaning of corroded iron artefacts using pulsed TEA CO_2- and Nd:YAG-lasers, J. Cult. Herit., 4, 129s–133s.

[13] C.Fotakis, D.Anglos, V.Zafiropulos, S.Georgiou, V.Tornari (2007) Lasers in the Preservation of Cultural Heritage: Principles and Applications, first ed., Taylor & Francis Group, Boca Raton.

[14] R.Pini, S.Siano, R.Salimbeni, M.Pasquinucci, M.Miccio (2000) Tests of laser cleaning on archeological metal artefacts, J. Cult. Heritage, 1, S129–S137.

[15] B.M.Radojković, S.S.Ristić, S.R.Polić, R.M.Jančić-Heinemann, D.Radovanović (2017) Preliminary investigation on the use of the Q-switched Nd:YAG laser to clean corrosion products on museum embroidered textiles with metallic yarns, J. Cult. Herit., 23, 128-137.

[16] P.Mottner, G.Wiedemann, G.Haber, W.Conrad, (2003) A.Gervais Laser Cleaning of Metal Surface - Laboratory Investigations, Lasers in the Conservation of Artworks, LACONA V 79-86.

[17] B.V.Jegdić, S.R.Polić-Radovanović, S.S.Ristić, A.B.Alil (2012) Corrosion stability of corrosion products on an archaeological iron artifact, Int. J. Conserv. Sci., 3, 241-248.

[18] P.Pasquet, R.del Coso, J.Boneberg, P.Leiderer, R.Oltra, J.P.Boquillon (1999) Laser cleaning of

oxide iron layer: Efficiency enhancement due to electrochemical induced absorptivity change, Appl. Phys. A-Mater., 69, S727–S730.
[19] P.Dillmann, G.Béranger, P.Piccardo, H.Matthiesen (Eds) (2007) Corrosion of metallic heritage artefacts, CRC Press, Boca Raton, USA.
[20] J.R.Scully (2005) Electrochemical test, in: R.Baboian (Ed.), Corrosion test and standards: Application and interpretation, ASM International, West Conchohocken, USA, p. 107-130.
[21] Standard test method for conducting potentiodynamic polarisation resistance measurements-ASTM G59.
[22] M.E.Orazem, B.Tribollet (2008) Electrochemical impedance spectroscopy, first ed., John Wiley and Sons, New Jersey.
[23] M.G.Fontana, R.W.Staehle (1976) Advances in corrosion science and technology, Vol 6, Plenum Press, New York, London.
[24] Standard practice for calculation of corrosion rates and related information from electrochemical measurements-ASTM G102.
[25] R.Baboian (2002) NACE Corrosion Engineer's Reference Book, NACE International, Houston, Texas.
[26] R.Vilar (2012) Laser surface modification of steel and cast iron for corrosion resistance, in: C.T.Kwok (Eds.), Laser surface modification of alloys for corrosion and erosion resistance, Woodhead Publishing Limited, Oxford, p. 3-40.
[27] A.C.Agudelo, J.R.Gancedo, J.F.Marco, M.F.Creus, E.Gallego-Lluesma, J.Desimoni, R.C.Mercader (1999) Characterization and corrosion studies of laser-melted carbon steel surfaces, Appl. Surf. Sci., 148, 171–182.
[28] C.S.Dong, Y.Gu, M.L.Zhong, L.Li, M.X.Ma, W.J.Liu (2011) The effect of laser remelting in the formation of tunable nanoporous Mn structures on mild steel substrates, Appl. Surf. Sci., 257, 2467-2473.
[29] D.Loveday, P.Peterson, B.Rodgers (2004) Evaluation of Organic Coatings with Electrochemical Impedance Spectroscopy, Part 2: Application of EIS to Coatings, JCT Coat. Tech., 10, 88–93.
[30] D.Loveday, P.Peterson, B.Rodgers (2005) Evaluation of Organic Coatings with Electrochemical Impedance Spectroscopy, Part 3: Protocols for Testing Coatings with EIS, JCT Coat. Tech., 2, 22–27.
[31] B.V.Jegdić, J.B.Bajat, J.P.Popić, S.I.Stevanović, V.B.Mišković-Stanković (2011) The EIS investigation of powder polyester coatings on phosphated low carbon steel: The effect of NaNO2 in the phosphating bath, Corros. Sci., 53, 2872-2880.
[32] Lj.S.Živkovič, B.V.Jegdić, J.P.Popić, J.B.Bajat, V.B.Mišković-Stanković (2013) The influence of Ce-based coatings as pretreatments on corrosion stability of top powder polyester coating on AA6060, Prog. Org. Coat., 76, 1387-1395.
[33] B.V.Jegdić, Lj.S.Živković, J.P.Popić, J.Rogan, J.B.Bajat, V.B.Mišković-Stanković (2016) Corrosion stability of cerium-doped cataphoretic epoxy coatings on AA6060 alloy, Mater. Corros., 67, 1173-1184.

IZVOD

KOROZIONA SVOJSTVA LASERSKI ČIŠĆENIH POVRŠINA NA ARTEFAKTU OD GVOŽĐA

U ovom radu, Nd:YAG laser je korišćen za čišćenje površina artefakata od gvožđa koji su bili prekriveni korozionim produktima. Korozioni produkti su uklonjeni bez oštećivanja osnovnog materijala. Za određivanje brzine korozije mehanički čišćene površine, laserski čišćene površine i laserski čišćene površine na koju je nakon čišćenja nanesen zaštitni sloj Paraloid B44, korišćene su tri različite elektrohemijske metode. Morfologija čišćenih površina je ispitivana SEM mikroskopijom. Metoda linearne polarizacione otpornosti, elektrohemijska impedansna spektroskopija i voltametrija sa linearnom promenom potencijala pokazale su da je brzina korozije laserski čišćene površine uzorka od gvožđa za oko 50% veća od brzine korozije mehanički čišćene površine. Elektrohemijska impedansna spektroskopija je pokazala da otpornost pora Paraloid prevlake na laserski čišćenoj površini uzorka opada na početku ispitivanja nakon čega dostiže konstantnu vrednost. Na početku ispitivanja, vrednost otpornosti razmeni elektrona je konstantna nakon čega naglo opada, tj. brzina korozije gvožđa u porama Paraloid prevlake raste sa vremenom. Tokom ispitivanja tehnikom voltametrije sa linearnom promenom potencijala na uzorku od gvožđa sa Paraloid prevlakom, zapaženo je da anodna kriva polarizacije ima neuobičajen oblik pri potencijalima pozitivnijim od - 0.5 V.

Ključne reči: *artefakti od gvožđa, lasersko čišćenje, korozija, elektrohemijske metode, brzina korozije.*

Naučni rad
Rad primljen: 10. 11. 2019.
Rad prihvacen: 04. 12. 2019.
Rad je dostupan na sajtu: www.idk.org.rs/casopis